MASTER

HEDL-SA-1906
CONF-791058--44

A COUPLED CHANNELS MODEL FOR RADIATIVE CAPTURE OF NUCLEONS BY ^{12}C.

D.L. Johnson

DISCLAIMER

This book was prepared as an account of work sponsored by an agency of the United States Government. Neither the United States Government nor any agency thereof, nor any of their employees, makes any warranty, express or implied, or assumes any legal liability or responsibility for the accuracy, completeness, or usefulness of any information, apparatus, product, or process disclosed, or represents that its use would not infringe privately owned rights. Reference herein to any specific commercial product, process, or service by trade name, trademark, manufacturer, or otherwise, does not necessarily constitute or imply its endorsement, recommendation, or favoring by the United States Government or any agency thereof. The views and opinions of authors expressed herein do not necessarily state or reflect those of the United States Government or any agency thereof.

International Conference
on Cross Sections

October 22-26, 1979 Knoxville, TN

HANFORD ENGINEERING DEVELOPMENT LABORATORY
Operated by Westinghouse Hanford Company, a subsidiary of
Westinghouse Electric Corporation, under the Department of
Energy Contract No. DE-AC14-76FF02170

COPYRIGHT LICENSE NOTICE
By acceptance of this article, the Publisher and or recipient acknowledges the U.S. Government's right to retain a nonexclusive, royalty free license in and to any copyright covering this paper.

DISTRIBUTION OF THIS DOCUMENT IS UNLIMITED

DISCLAIMER

This report was prepared as an account of work sponsored by an agency of the United States Government. Neither the United States Government nor any agency Thereof, nor any of their employees, makes any warranty, express or implied, or assumes any legal liability or responsibility for the accuracy, completeness, or usefulness of any information, apparatus, product, or process disclosed, or represents that its use would not infringe privately owned rights. Reference herein to any specific commercial product, process, or service by trade name, trademark, manufacturer, or otherwise does not necessarily constitute or imply its endorsement, recommendation, or favoring by the United States Government or any agency thereof. The views and opinions of authors expressed herein do not necessarily state or reflect those of the United States Government or any agency thereof.

DISCLAIMER

Portions of this document may be illegible in electronic image products. Images are produced from the best available original document.

1906

A COUPLED CHANNELS MODEL FOR RADIATIVE CAPTURE OF NUCLEONS BY ^{12}C.

D. L. Johnson†

University of Washington
Seattle, Washington 98195 USA

A simple model based upon coupled channels scattering calculations for nucleons on ^{12}C has been applied to the corresponding radiative capture reactions. It includes only electric dipole transitions via direct capture plus capture occurring via intermediate states consisting of only the 2+ first excited state of ^{12}C coupled to a nucleon in the s,d shell. It is shown that the shape and magnitude of measured excitation functions of the $^{12}C(p,\gamma_0)$ and $^{13}C(\gamma,n_0)$ reactions are largely reproduced for excitation energies up to about 10 MeV. Furthermore, it is shown that the excitation functions are strongly affected by competition and interference between direct capture and the indirect modes. Angular distribution data is also fairly well reproduced by the model. Implications of the success of the model will be discussed.

[Nuclear reactions, $^{12}C(p,\gamma_0)^{13}N$, $d\sigma(E_p,\theta)/d\Omega$ E_p <9 MeV, $^{13}C(\gamma,n_0)^{12}C$, $d\sigma(E_\gamma,\theta)/d\Omega$, E_γ<10 MeV, coupled channels model calculation, comparison to experimental data]

Introduction

There is a continuing need for development of simple nuclear models that can be applied to the understanding, prediction, and evaluation of nuclear reaction data. Here the interest was primarily in explaining data on the capture of low energy nucleons by ^{12}C.

For applied purposes, data on neutron capture by ^{12}C can be useful because, for example, (1) carbon is used in fission and fusion reactors, (2) carbon is a standard for neutron cross section measurements, (3) carbon is used in organic neutron detectors, and (4) the $^{13}C(\gamma,n)$ reaction provides a neutron source that must be considered under certain circumstances. Proton capture data may be useful for example in astrophysics.

A simple model was applied to describe the radiative capture of either neutrons or protons that was based upon coupled channels calculations which had previously been used to describe their scattering by ^{12}C. The model was very successful as will be shown and explained several complex features of experimental data.

It was somewhat surprising to see such good agreement however. Despite the successful application of the coupled channels approach to scattering, it was by no means clear that it should work as well for radiative capture. For example, weak configurations in the continuum wave functions that are neglected in the simple model might have a profound effect upon capture. The most important of these neglected configurations was expected to be that involving the giant dipole resonance of the target nucleus coupled to a single nucleon, such as is included in the so-called direct-semi-direct (DSD) capture model (Ref. 1).

The relevant structure of ^{12}C and mass 13 nuclei will be discussed. Then the data relating to capture will be described and following that, the model and its results. Finally, implications of the model will be discussed.

Relevant levels of ^{12}C and A=13 Nuclei

Radiative capture of a nucleon by ^{12}C leads to either of the mirror nuclei ^{13}C or ^{13}N. The low energy levels of these nuclei are shown in Figure 1. Shown on either side are the energy levels of ^{12}C to which each of the compound systems can decay by emission of a nucleon. Also shown are the laboratory energy scales for incident neutrons or protons which correspond to a given excitation energy in the compound system or to the threshold for inelastic scattering to a level in ^{12}C.

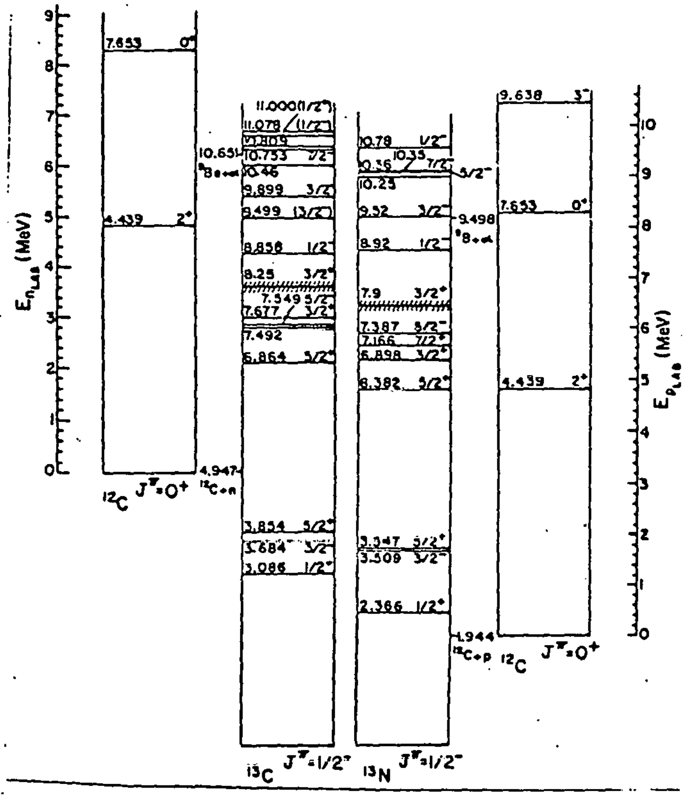

Fig. 1. Low energy level structure of A = 13 nuclei.

The proton capture reaction can be described entirely by radiative transitions to the ground state since all other states are unbound to proton decay and therefore cascade transitions cannot contribute significantly. Neutron capture can involve transitions to the three bound excited states shown, however, most of the applicable data is actually for the inverse $^{13}C(\gamma,n)$ reaction which involves only the ground state of ^{13}C. The cross section for the $^{13}C(\gamma,n_0)^{12}C$ reaction is easily related by detailed balance to that of the $^{12}C(n,\gamma_0)^{13}C$ reaction. One expects a great deal of similarity in the two capture reactions because of the high degree of symmetry between the mirror nuclei.

The primary interest will be in neutron capture for incident energies less than ~ 5 MeV($E_\gamma \gtrsim$ 9.4MeV) and proton capture for energies less than ~8 MeV because only elastic scattering and inelastic scattering to the 2+ first excited state of ^{12}C, and radiative capture reactions are possible. Furthermore, below about 10MeV in excitation, in mass 13, the structure of the positive parity states is very simple and well understood.

Detailed shell model calculations (ref. 2) have confirmed that below ~ 10 MeV the positive parity states are composed almost entirely of the 0+ and 2+ states weakly coupled to single s,d shell nucleons, however, some mixing of configurations occurs and the 1/2+,3/2+, 5/2+, and 9/2+ states from the $(2+ \otimes d_{5/2})$ configuration that would normally occur at ~ 8 MeV are pushed to energies greater than 10 MeV.

Capture and Photonuclear Data

There have been several measurements of the capture reaction for protons less than ~3 MeV, but only one measurement is known for the range of ~3 to 9 MeV. (Ref. 3). Figure 2 shows measured excitation functions at 90° for both the (p,γ_0) and the $(p,p'\gamma)$ (4.44MeV) reactions.

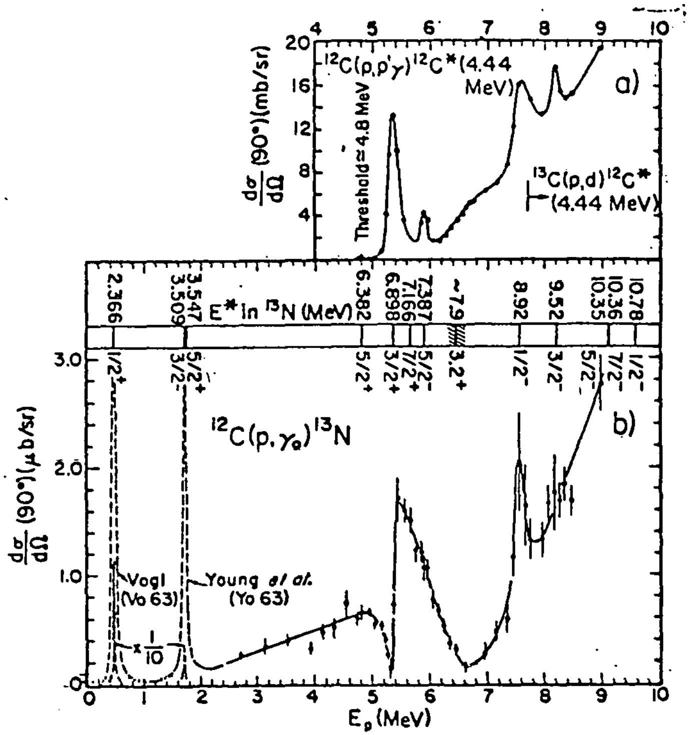

Fig. 2. Measured excitation functions of the differential cross-section at 90°. Lines are to guide the eye and are not based on theory.
a) The $^{12}C(pp'\gamma)^{12}C^*$(4.44 MeV) reaction.
b) The $^{12}C(p,\gamma_0)^{13}N$ reaction. Data from references 3, 4, and 5.

For the capture reaction data, one would expect E1 transitions to be very prominent. These would involve only 1/2+ or 3/2+ states in the compound system decaying to the 1/2 - ground state. Strong resonance effects are in fact seen that correspond to the 1/2+ state at 2.366 MeV and the 3/2+ state at 6.898 MeV in ^{13}N. Surprisingly, a minimum is seen near the only other possible E1 candidate, the broad 3/2+ state at ~7.9 MeV. A strong resonance is seen in the inelastic scattering at the lower 3/2+ state indicating that the capture reaction might also have effects associated with excitation of the 2+ state. The only other capture resonances correspond to the first 3/2- state at 3.509 MeV and the first 1/2- state at 8.52 MeV. Both of these resonances involve predominantly M1 transitions. The other compound states are not expected to be significant in capture because they would correspond to M1 multipolarity or higher and are in general rather narrow.

Since a significant capture cross-section was observed between resonances, (in particular in the wide space between ~ 3.5 to ~ 6.4 MeV in excitation), an important direct capture contribution was suggested. For direct capture, E1 radiation should predominate over higher multipoles. Thus it appears that aside from the two M1 resonances, the excitation function for capture of protons less than ~ 9 MeV is associated with E1 radiation via direct and resonant mechanisms.

There have been several measurements of the $^{13}C(\gamma,n)$ reaction at low energies. The most detailed data available at the time of this work was that of Bertozzi et al, (Ref. 6) which is shown in Figure 3. Note that the excitation function at 77° is quite similar in shape to the (p,γ_0) excitation function at 90°.

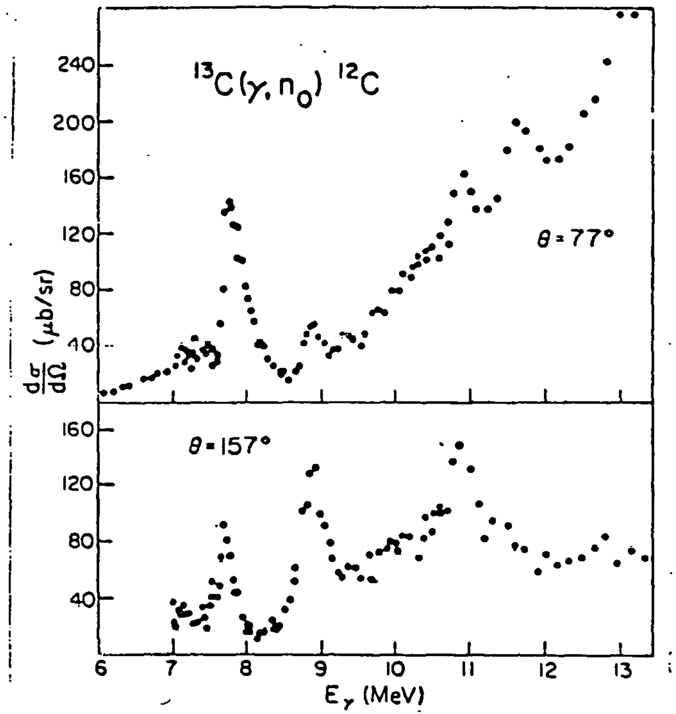

Fig. 3. Measured excitation functions of the $^{13}C(\gamma,n_0)^{12}C$ reaction. Data are taken from Bertozzi et al. (Ref. 6).

The data of Bertozzi et al, were quite useful for the theoretical comparisons to be discussed. It was known that E1 capture or photoemission involving the ground state has an angular distribution that can be described with only two terms in a Legendre expansion.

$$\frac{d\sigma}{d\Omega}(\theta) = A_o\,(1 + a_2P_2(\cos\theta)) \qquad (1)$$

Therefore it was possible to solve for the total cross section ($4\pi A_o$) and the a_2 coefficient at each energy in the excitation function where measurements at the two angles were made. Near the M1 resonance at ~9 MeV, there can be an additional $a_1P_1(\cos\theta)$ term in the angular distribution due to E1/M1 interference. Hence, this procedure was not used for energies near the 9 MeV resonance.

The Capture Model

The capture model is briefly outlined here, details may be found in Ref. 3. The cross section for radiative capture from a continuum state to a bound state is proportional to the square of the electromagnetic matrix element between the initial continuum wave function and the final bound state wave function.

Here the electric dipole operator was used and wave functions for only the 1/2+ and 3/2+ incident channels were needed.

The initial continuum wave functions were provided by solution of a coupled channels optical model calculation of the scattering of nucleons by ^{12}C.

The incident wave function corresponding to the $J^{\pi}=3/2+$ channel can be written in the following short hand notation which represents the presence of excited core states.

$$\psi_i(3/2^+) = (0^+ \otimes d_{3/2})^{3/2+} + (2^+ \otimes s_{1/2})^{3/2^+} + (2^+ \otimes d_{5/2})^{3/2+} + (2^+ \otimes d_{3/2})^{3/2^+} \qquad (2)$$

For each configuration in the expansion, the coupled nucleon has a different radial wave function which varies with the incident energy. The expansion for the $1/2^+$ incident channel is analogous.

The coupled-channels scattering calculations of Mikoshiba, Tanifuji, and Terasawa (Ref. 7) have been reproduced in this work in order to generate the continuum wave functions. Their view was that the 0^+ and 2^+ states were the lowest states in the ground state rotational band of an oblate deformed ^{12}C nucleus. ($\beta = -0.5$). Excitation of the 2^+ state was treated phenomenologically via an interaction of the incident nucleon with the non-spherical part of a deformed oblate optical potential. A great deal of effort was made by Mikoshiba, et al., to reproduce the excitation functions of proton elastic and inelastic scattering cross sections and to give the correct locations for positive parity resonances below about 10 MeV in ^{13}N. In order to fit the resonant states, the real optical potential describing the interaction of a nucleon with ^{12}C was allowed to depend slightly upon the nucleon energy. In addition, a spin orbit potential and very weak spin-spin and (ℓ^2) orbital angular momentum dependent interactions were incorporated. No imaginary potential was used because all scattering channels were explicitly included. The scattering of neutrons by ^{12}C was then described using the same potential, after removing the coulomb term.

The wave function of the ground state of either ^{13}N or ^{13}C must be expanded in the same weak coupling form as the incident wave function for use in capture calculations. It has been shown (Ref. 8) that the ground state expansion includes many ^{12}C core states coupled to p-shell nucleons. The largest configurations involve the 0^+ ground state, 2+ states at 4.44 and 16.1 MeV, and 1^+ states at 12.7 and 15.1 MeV. However, only configurations involving the 0^+ and 2^+ first excited states coupled to p-shell nucleons can couple via E1 radiation to the simple continuum wave functions that have been considered. The important parts of the ground state wave function can be written as

$$\psi_f(1/2^-) = \theta_1(0^+ \otimes P_{1/2})^{1/2^-} + \theta_2(2^+ \otimes P_{3/2})^{1/2^+} + \ldots \qquad (3)$$

Here θ_1 and θ_2 are expansion coefficients which are related to the spectroscopic factor for each configuration.

The radial wave functions for each of the bound configurations were calculated using a Woods-Saxon form and a spin orbit term. The same radius, diffuseness, spin orbit, and coulomb potential parameters were used as for the coupled channels scattering calculations, however, the depth of the potential was adjusted to reproduce the binding energy of a single nucleon for each configuration. The binding energy of a nucleon coupled to the 2^+ state was taken to be 4.44 MeV more than the normal ground state binding energy.

The expansion parameters of the ground state wave function were taken from spectroscopic factors calculated by Cohen and Kurath (Ref. 8), whose results have been shown to be in good agreement with a wide variety of experimental data for p-shell nuclei. The values were $\theta_1 = 0.783$ and $\theta_2 = 1.059$, hence the probabilities for each configuration were comparable.

An example of the radiative capture mechanism is shown schematically in Figure 4. Here one sees a $d_{3/2}$ proton incident upon the 0^+ target. After collision, a compound system is formed with a wave function as in equation 2. Each of the configurations in the compound system can radiate via E1 single particle transitions to a configuration in the $1/2^-$ ground state with the core states of ^{12}C acting only as spectators. Direct capture takes place via radiative decay of the $d_{3/2}$ nucleon to a bound $p_{1/2}$ orbital. A similar process occurs for capture via the $1/2^+$ incident channel.

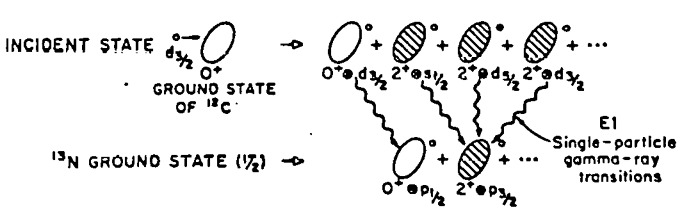

Fig. 4. Schematic diagram of the $^{12}C(p,\gamma_o)^{13}N$ reaction involving coupled-channels capture via excitation of the 2^+ first excited state of ^{12}C. Incident channel is $J^{\pi} = 3/2^+$.

It can be shown that the cross section for E1 capture to the ground state can be written as

$$\sigma = \frac{4K\gamma}{3\hbar\, v_1}[M_{1/2^+}^2 + 2M_{3/2^+}^2] \qquad (4)$$

where $M_{1/2^+}$ and $M_{3/2^+}$ are the reduced matrix elements for E1 transitions via either the $1/2^+$ or $3/2^+$ incident channels, $K\gamma$ is the photon wave number, and v_1 is the relative velocity of the incident nucleon and the target. Furthermore, because of the wave functions, each matrix element is expressed as the sum of several coherent contributions as in Figure 4. For the $3/2^+$ channel, the matrix element can be written as

$$M_{3/2^+} = \langle 3/2^+|E1|\ 1/2^-\rangle = \Theta_1 A_1 + \Theta_2 A_2 + \Theta_2 A_3 + \Theta_2 A_4 \qquad (5)$$

where Θ_1 and Θ_2 are the ground state expansion parameters and the A's are partial amplitudes for each of the E1 single particle transitions in Figure 4. For example, $A_4 = \langle 2^+ \otimes s_{1/2}|E1|2^+ \otimes p_{3/2}\rangle$

Interference effects may be expected between the transitions contributing to each of the reduced matrix elements.

The angular dependence was also calculated for both capture and photonuclear reactions. For pure E1 capture, the angular distribution has the form shown in equation 1. The a_2 coefficient can be expressed as

$$a_2 = \frac{2\mathrm{Re}(M_{1/2}{}^* M_{3/2}) - M_{3/2}^2}{M_{1/2}^2 + 2\, M_{3/2}^2} \qquad (6)$$

This coefficient is sensitive to the ratio of capture proceeding via either the $1/2^+$ or $3/2^+$ incident channels. The first term in the numerator is related to E1/E1 interference between transitions via the two incident channels. If one ignores this term then the a_2 coefficient is bounded between $a_2 = 0.0$ (isotopic) for capture solely via $1/2^+ \rightarrow 1/2^-$ transitions and $a_2 = -0.5$ for capture solely via $3/2^+ \rightarrow 1/2^-$ transitions. The effect of the interference term could give an a_2 coefficient outside these limits.

Results

Calculations of the radiative capture cross section were made for protons up to 9 MeV and for neutrons up to 6 MeV using the model described above. The results for proton capture evaluated at 90° are compared to the experimental data between 2.7 and 9 MeV in Figure 5. The agreement is excellent except for the two M1 resonances shown in Figure 2, which are not included in the model resonance. The parameters used in the model appear to be near optimal. Some studies of the sensitivity to these parameters have been done but will not be presented here.

Results of calculations of the neutron capture cross section are shown in Figure 6. The shape is quite similar to that for proton capture, as expected, except for the low energy (p,γ) resonances that cannot occur in neutron capture.

The results of calculations of the (γ,n_0) cross section are compared to a sampling of experimental data in Figure 7. Agreement is not quite as good as for the p,γ_0 reaction, however, it is believed that small changes in the model would give excellent agreement.

To examine what determines the shape of the calculated cross section, the contributions from each of

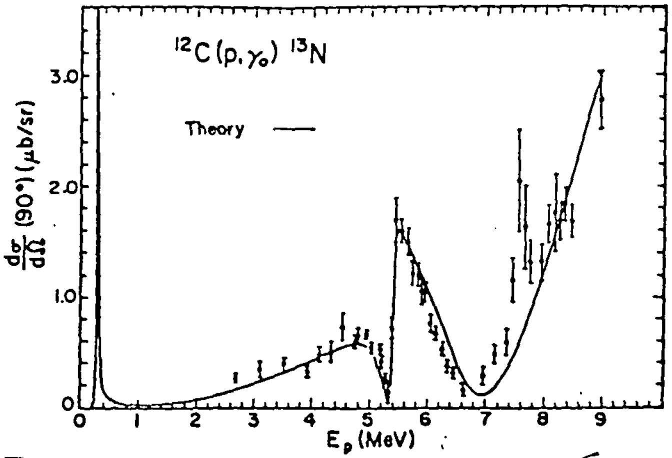

Fig. 5. $^{12}C(p,\gamma_0)^{13}N$ reaction. Comparison of calculated and measured excitation function at 90°. Data from 2.7 to 9 MeV only (Ref. 3).

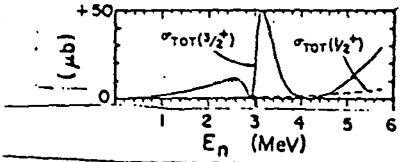

Fig. 6. $^{12}C(n,\gamma_0)^{13}C$ reaction. Calculated cross sections for $1/2^+$ and $3/2^+$ incident channels.

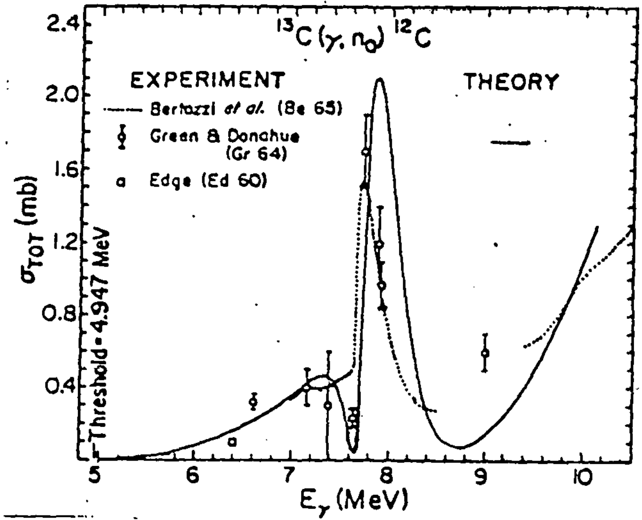

Fig. 7. $^{13}C(\gamma,n_0)^{12}C$ reaction. Comparison of calculated and measured cross-sections.

the transitions involved in the $3/2^+$ incident channel are shown separately in Figure 8 along with interference effects. The total contribution from capture via the $1/2^+$ incident channel is also shown but is small except for the low energy resonance which is predominantly direct capture via an $s_{1/2} \rightarrow p_{1/2}$ transition. Cross sections for capture via the transitions shown in Figure 4 are labeled 1 to 4. Curves labeled by two numbers correspond to the effects of interference between two transition channels.

The direct capture contribution (channel 1) is seen as a broad resonance centered near a proton energy where one expects a potential scattering resonance in the elastic $d_{3/2}$ channel. However, a strong dip is seen in this contribution due to competition effects associated with a resonance in the $(2^+ \otimes s_{1/2})^{3/2^+}$ configuration of the incident wave function. Note that

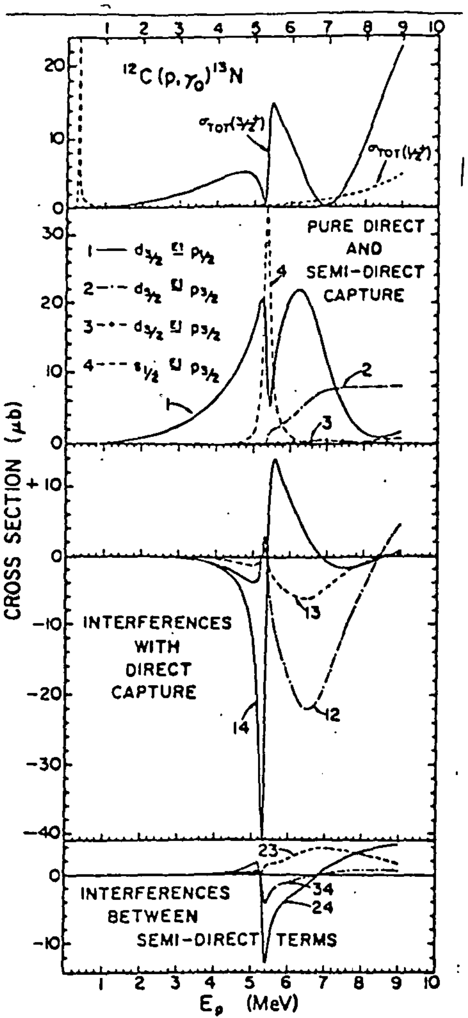

Fig. 8. $^{12}C(p,\gamma_0)^{13}N$ reaction. Shown are contributions due to pure direct capture, semi-direct capture, and the interferences between them (only capture via the $3/2^+$ incident channel is broken down).

the direct capture contribution is not at all like experimental observations.

Capture that proceeds via the inelastic configurations has a profound effect upon the shape and magnitude of the excitation function. For example, the strong interference minimum seen for protons of ~5.3 MeV is caused by interference between direct capture and capture via the $(2^+ \otimes s_{1/2})^{3/2^+} \rightarrow (2^+ \otimes p_{3/2})^{1/2^-}$ transition (channel 4). Also, the broad minimum for protons of ~ 7 MeV is due mainly to interference between direct capture and the $(2^+ \otimes d_{5/2})^{3/2^+} \rightarrow (2^+ \otimes p_{3/2})^{1/2^-}$ transition (channel 2). Furthermore, the rise in cross section at higher energies is caused predominantly by capture via the $(2^+ \otimes d_{5/2}) \rightarrow (2^+ \otimes p_{1/2})$ transition (channel 2) plus constructive interferences between it and the other inelastic capture channels. At the lowest energies, the direct mechanism dominates as might be expected.

The a_2 coefficient of the angular distribution was calculated for both the (p,γ_0) and (γ,n_0) reactions. The results are compared in Figure 9 to the values derived from the (γ,n_0) data of Bertozzi, et al.(Ref.6) described earlier. Note that the a_2 coefficient varies significantly with energy, indicating the changes in the ratio of transitions via the $1/2^+$ continuum channel compared to the $3/2^+$ channel. Since the a_2 coefficient exceeds the limits of 0 and -0.5 described earlier, it reflects the interference between the two E1 modes. The calculated a_2 coefficient is considered to be in fairly good agreement with the experimental data which are of unknown quality.

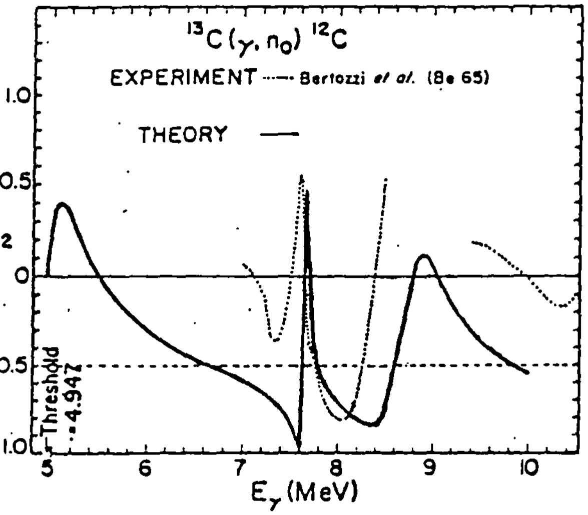

Fig. 9. $^{13}C(\gamma,n_0)^{12}C$ reaction. Comparison of calculated a_2 coefficient to experimental results.

Discussion

Considering the complexity of the competion and interference effects, it is surprising that the shape and magnitude of the experimental data are so well reproduced. It is apparent that the coupled channels calculations of Mikoshiba, et al. (Ref. 7) provide an excellent description of the important continuum wave functions.

The success of the model seems to imply that weak configurations in the continuum wave functions that were neglected are not important for capture at these low energies. One might expect a small probability for configurations such as $(1^+ \otimes s_{1/2})^{3/2^+}$ in the continuum wave function where the 1^+ state is either the 12.71 MeV (T=0) or the 15.1 MeV (T=1). Such configurations could radiate to the ground state via E1 single particle transitions just like the ones considered. However, one would not expect such configurations to become important until higher energies in the weak coupling view. Furthermore, the transition amplitudes would tend to be small because of the deep binding of the nucleon coupled to the highly excited core state in the ground state configuration.

A more important configuration for E1 capture might be expected from a configuration in the compound system having the giant dipole resonance of ^{12}C coupled to a p-shell nucleon (e.g. $(1^- \otimes p_{1/2})^{3/2^+}$). Such a configuration could radiate strongly to the ground state because of collective E1 enhancement even when only a small admixture is present in the compound system. It is explicitly included in the so-called DSD model (Ref. 1). It can be shown that at low energies, the effects of the coupled channels mechanism are dominant over the DSD mechanism because of a large overlap of radial wave functions external to the compound system which does not occur for the DSD mechanism.

Another way of viewing the simple mechanism described is from the point of view of photonuclear reactions. It is well known that for light nuclei away from closed shells, there is considerable E1 strength below the main dipole states at ~ 20 MeV. The broad pygmy resonance in mass 13 nuclei at ~ 13 MeV is a good example of this effect. Note that the model described here predicts the lower part of the pygmy resonance to be associated primarily with the $(2^+ \otimes d_{5/2})^{3/2+}$ configuration in the continuum.

One would therefore expect that capture involving low lying excited target states might be applicable at low energies for other light targets that do not lead to closed shells. For example, the $^{17}O(\gamma,n)$ reaction at low energy (Ref. 11) shows effects very similar to those seen here including a significant resonant dip that might be explained as the effect of competition or interference between modes involving various core states. Note that a similar coupled channels model was developed by Buck and Hill (Ref. 12) to treat photonuclear reactions on closed shell nuclei. Some success was obtained for ^{16}O. A significant difference was that here a complex wave function was used for the ground state.

The model described here has similarities to the valence model (Ref. 13) in that a significant portion of the capture occurs via the direct transition and is correlated with the nucleon width. It is also similar to the DSD model (1) in that core excited states are involved, however, here the coupled single nucleons decay rather than the core state. It is also similar to a compound nuclear mechanism in which only the first stage of core excitation is involved. Note that resonances such as the first $1/2^+$ state in ^{13}N have been treated as compound nuclear effects (Ref. 14) with an underlying direct component, however, in the present model it is predominantly a direct capture resonance.

Work supported in part by the U.S.A.E.C. (at (45-1) -1388, Prog. A).

†Present address: Westinghouse Hanford Company,
Richland, Washington 99352

References

1. G.E. Brown, Nucl. Phys. 57 (1964) 339.
2. H.U. Jäger, H.R. Kissener, and R.A. Eramzhian. Nucl. Phys. A171 (1971) 16.
3. D.L. Johnson, Phd. Dissertation, University of Washington (1974), unpublished.
4. J.L. Vogl, Phd. Dissertation, California Institute of Technology (1963), unpublished.
5. F.C. Young, J.C. Armstrong, and J.B. Marion. Nucl. Phys. 44 (1963) 486.
6. W. Bertozzi, P.T. Demos, S. Kowalski, F.R. Paolini, C.P. Sargent, and W. Turchinetz. Nucl. Instr. and Meth. 33 (1965) 199.
7. O. Mikoshiba, T. Terasawa, and M. Tanifuji. Nucl. Phys. A168 (1971) 417.
8. S. Cohen and D. Kurath. Nucl. Phys. A101 (1967) 1.
9. L. Green and D.J. Donahue. Phys. Rev. 135 (1964) B701.
10. R.D. Edge, Phys. Rev. 119 (1960) 1643.
11. R.J. Holt, H.E. Jackson, R.M. Laszewski, J.E. Monahan, and J.R. Specht. ANL-78-66 (ANL Physics Div. Annual Report) pg. 116.
12. B. Buck and A.D. Hill. Nucl. Phys. A95 (1967) 271.
13. J.E. Lynn. Theory of Neutron Resonance Reactions, Oxford Univ. Press. (1968) pg. 326.
14. C. Rolfs and R.E. Azuma, Nucl. Phys. A227 (1974) 291.